GEODESY AND GEODYNAMICS 2015, VOL 6 NO 1, 46–54

Available online at www.sciencedirect.com
ScienceDirect
journal homepage: www.keaipublishing.com/en/journals/geog;
http://www.jgg09.com/jweb_ddcl_en/EN/volumn/home.shtml

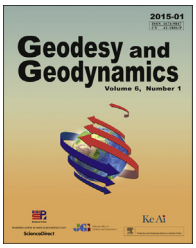

Numerical simulation of influences of the earth medium's lateral heterogeneity on co- and post-seismic deformation

Xu Bei[a], *Xu Caijun*[a,b,*]

[a] *School of Geodesy and Geomatics, Wuhan University, Wuhan 430079, China*
[b] *Collaborative Innovation Center of Geospatial Technology, Wuhan 430079, China*

ARTICLE INFO

Article history:
Received 30 August 2014
Accepted 15 November 2014
Available online 23 March 2015

Keywords:
Finite element method
Medium's lateral heterogeneity
Numerical simulation
Co-seismic deformation
Post-seismic deformation
Geodynamics
Viscosity coefficient
Model construction

ABSTRACT

Many studies revealed that the Earth medium's lateral heterogeneity can cause considerable effects on the co- and post-seismic deformation field. In this study, the three-dimensional finite element numerical method are adopted to quantify the effects of lateral heterogeneity caused by material parameters and fault dip angle on the co- and post-seismic deformation in the near- and far-field. Our results show that: 1) the medium's lateral heterogeneity does affect the co-seismic deformation, with the effects increasing with the medium's lateral heterogeneity caused by material parameters; 2) the Lame parameters play a more dominant role than density in the effects caused by lateral heterogeneity; 3) when a fault's dip angle is smaller than 90°, the effects of the medium's lateral heterogeneity on the hanging wall are greater than on the footwall; 4) the impact of lateral heterogeneity caused by the viscosity coefficient on the post-seismic deformation can affect a large area, including the near- and far-field.

1. Introduction

The rapid development of modern space geodetic techniques and the study of dislocation theory have brought new opportunities to seismological research. The finding that most tectonic earthquakes occur on faults is one of the largest advances in seismology in the 20th century. Steketee [1] first introduced the dislocation theory to seismology, and since then, dislocation theory has seen significant development. Chinnery [2,3] derived the expressions for the surface displacements and stress near vertical strike-slip faults; Maruyama [4] extended these expressions to dip-slip faults. Chen et al. [5,6] discussed the general inversion method with semi-infinite space dislocation theory and ground deformation data, and inverted the source processes of the 1966 Xingtai earthquake and the 1976 Tangshan earthquake.

* *Corresponding author*. School of Geodesy and Geomatics, Wuhan University, Wuhan 430079, China.
E-mail address: cjxu@sgg.whu.edu.cn (Xu C.).
Peer review under responsibility of Institute of Seismology, China Earthquake Administration.

Production and Hosting by Elsevier on behalf of KeAi

http://dx.doi.org/10.1016/j.geog.2014.11.001

Okada [7] reviewed and analyzed the closed analytical expressions that describe the surface deformation due to shear faulting in a half-space, and presented a suite of expressions for the surface displacements, strains, and tilts due to inclined shear and tensile faults in a half-space for both point and finite rectangular sources. Wang et al. [8] attempted to develop the formulations in a more realistic earth model, which includes the effect of crustal layering.

However, a realistic earth model is very complex, possessing not only crustal layering but also medium lateral heterogeneity, such as is found in the Longmenshan Mountains area [9–11]. According to Rybicki et al. [12–14], lateral heterogeneity can sometimes cause considerable effects on the co-seismic deformation fields. Li et al. [15] demonstrated, using numerical simulation, that the medium's lateral heterogeneity has influences on the co-seismic deformation. However, issues such as how the medium's lateral heterogeneity affects co- and post-seismic displacements, which parameters control the effects, whether a fault's dip angle has influences on the effects, and whether the effects are the same in the near- and far-field are yet to be addressed sufficiently. In this study, using numerical simulation through detailed analysis, we present the effects of the medium's lateral heterogeneity on the co- and post-seismic deformation fields in detail.

2. Model construction

A finite element model was constructed in the Cartesian coordinate system. The intersection of the fault plane and surface coincides with the Y-axis; the X-axis is perpendicular to the Y-axis and the Z-axis is perpendicular to the OXY plane. The region of the finite element model is: $-200\ \text{km} \le X \le 200\ \text{km}$, $-200\ \text{km} \le Y \le 200\ \text{km}$, $-310\ \text{km} \le Z \le 0\ \text{km}$. In the case of vertical strike-slip faults, the region of the fault is:$X = 0$ km, $0\ \text{km} \le Y \le 20\ \text{km}$, $-20\ \text{km} \le Z \le 0\ \text{km}$. After designing the region and slip distribution, the fault plane was embedded into the finite element model. Then, the region was divided into connected tetrahedral mesh.

The finite element model was divided into three layers, the first layer being the upper crust, the second layer the lower crust, and the third layer the mantle. The upper crust was separated by a fault plane, which could be set to possess different material properties on both sides of the fault plane, causing it to become laterally inhomogeneous. In addition, we assumed the fault to only be present in the upper crust. For the co-seismic problem, the material is three-dimensional isotropic elastic, and can thus be described by only three material properties, λ, μ, and ρ; λ and μ are the Lame parameters. The values of all the parameters were from Dziewonski and Anderson's preliminary reference Earth model [16].

3. Simulation and analysis

3.1. Impact of λ on co-seismic deformation

To study the impact of λ, μ, ρ and the other parameters should be kept constant. Here, we kept μ as $2.7 \times 10^{10}\ \text{Nm}^{-2}$ in all the experiments. Ten groups of experiments, listed in Table 1, were designed. Each group had three cases; all the parameters of case 2 and case 3 were the same, except for λ; the value of λ in case 2 was the same as that of the footwall in case 1; the value of λ in case 3 was the same as that of the hanging wall in case 1.

The ten groups of experiments were designed to determine the impact of the medium's lateral heterogeneity caused by the λ on co-seismic deformation. As a consequence of the differences in the λ, the material in case 1 of each group was laterally heterogeneous. On the contrary, the material in case 2 and case 3 of each group was homogeneous. Therefore, subtracting the co-seismic displacements of case 2 from the co-seismic displacements of case 1 gave the impact of the medium's lateral heterogeneity, caused by the λ of the hanging wall, on the co-seismic deformation (Fig. 1). Likewise, subtracting the co-seismic displacements of case 3 from the co-seismic displacements of case 1 gave the impact of the medium's lateral heterogeneity, caused by the λ in the footwall, on the co-seismic deformation (Fig. 1).

Fig. 1(a) Impact of lateral heterogeneity caused by the λ of the hanging wall on the co-seismic deformation in the X-axis direction; 1(b) Impact of the hanging wall in the Y-axis direction; 1(c) Impact of the hanging wall in the Z-axis direction; 1(d) The square root of the impact of the hanging wall in all directions; 1(e) Impact of lateral heterogeneity caused by the λ of the footwall on the co-seismic deformation in the X-axis direction; 1(f) Impact of the footwall in the Y-axis direction; 1(g) Impact of the footwall in the Z-axis direction; 1(h) The square root of the impact of the footwall in all directions. In the figure, the X-axis and Y-axis represent the area of the area of the earthquake.

In the numerical simulation results, the impact of the medium's lateral heterogeneity caused by λ on the co-seismic deformation was different in the three directions of the surface coordinate system. In the experimental results for the 10th group, the biggest change in the X-axis, Y-axis, and Z-axis directions was 5.3 mm, 7.6 mm, and 9.0 mm, respectively. Moreover, the rate of the biggest change in the Z-axis direction was just 3.25%.

As shown in Table 1, the parameter of λ in the hanging wall varied from $3.75 \times 10^{10}\ \text{Nm}^{-2}$ to $6.0 \times 10^{10}\ \text{Nm}^{-2}$ in steps of $2.5 \times 10^{9}\ \text{Nm}^{-2}$. The co-seismic displacement was observed to increase with an increase in λ. In addition, the increments of the co-seismic displacements were not linear; they were diminishing.

3.2. Impact of μ on co-seismic displacement

To study the influence of μ, λ, ρ, and the other parameters should be kept constant. Here, λ was set at $4.0 \times 10^{10}\ \text{Nm}^{-2}$ in all the experiments. Ten groups of experiments, listed in Table 2, were designed. Each group had three cases; the parameters of case 2 and case 3 were the same, except for the μ; the value of μ in case 2 was the same as that of the footwall in case 1; the value of μ in case 3 was the same as that of the hanging wall in case 1.

The ten groups of experiments were designed to determine the medium's lateral heterogeneity caused by the μ on the co-seismic deformation. As a consequence of the differences of μ,

Table 1 – Parameter values.

Group	Case	Dip angle (°)	ρ (kg/m^3)	λ (10^{10} Nm^{-2})		μ(10^{10} Nm^{-2})
				Hanging wall	Footwall	
1st	Case 1	60	2600.0	3.75	3.50	2.70
	Case 2	60	2600.0	3.50	3.50	2.70
	Case 3	60	2600.0	3.75	3.75	2.70
2nd	Case 1	60	2600.0	4.00	3.50	2.70
	Case 2	60	2600.0	3.50	3.50	2.70
	Case 3	60	2600.0	4.00	4.00	2.70
3rd	Case 1	60	2600.0	4.25	3.50	2.70
	Case 2	60	2600.0	3.50	3.50	2.70
	Case 3	60	2600.0	4.25	4.25	2.70
4th	Case 1	60	2600.0	4.50	3.50	2.70
	Case 2	60	2600.0	3.50	3.50	2.70
	Case 3	60	2600.0	4.50	4.50	2.70
5th	Case 1	60	2600.0	4.75	3.50	2.70
	Case 2	60	2600.0	3.50	3.50	2.70
	Case 3	60	2600.0	4.75	4.75	2.70
6th	Case 1	60	2600.0	5.00	3.50	2.70
	Case 2	60	2600.0	3.50	3.50	2.70
	Case 3	60	2600.0	5.00	5.00	2.70
7th	Case 1	60	2600.0	5.25	3.50	2.70
	Case 2	60	2600.0	3.50	3.50	2.70
	Case 3	60	2600.0	5.25	5.25	2.70
8th	Case 1	60	2600.0	5.50	3.50	2.70
	Case 2	60	2600.0	3.50	3.50	2.70
	Case 3	60	2600.0	5.50	5.50	2.70
9th	Case 1	60	2600.0	5.75	3.50	2.70
	Case 2	60	2600.0	3.50	3.50	2.70
	Case 3	60	2600.0	5.75	5.75	2.70
10th	Case 1	60	2600.0	6.00	3.50	2.70
	Case 2	60	2600.0	3.50	3.50	2.70
	Case 3	60	2600.0	6.00	6.00	2.70

the material in case 1 of each group was laterally heterogeneous. On the contrary, the material in case 2 and case 3 of each group was homogeneous. Therefore, subtracting the co-seismic displacements of case 2 from the co-seismic displacements of case 1 gave the impact of the medium's lateral heterogeneity, caused by the μ of the hanging wall, on the co-seismic deformation (Fig. 2). Likewise, subtracting the co-seismic displacements of case 3 from the co-seismic displacements of case 1 gave the impact of the medium's lateral heterogeneity, caused by the μ of the footwall, on the co-seismic deformation (Fig. 2).

Fig. 2(a) Impact of lateral heterogeneity caused by the μ of the hanging wall on the co-seismic deformation in the X-axis direction; 2(b) Impact of the hanging wall in the Y-axis direction; 2(c) Impact of the hanging wall in the Z-axis direction; 2(d) The square root of the impact of the hanging wall in all directions; 2(e) Impact of lateral heterogeneity caused by the μ of the footwall on the co-seismic deformation in the X-axis direction; 2(f) Impact of the footwall in the Y-axis direction; 2(g) Impact of the footwall in the Z-axis direction; 2(h) The square root of the impact of the footwall in all directions. In the figure, the

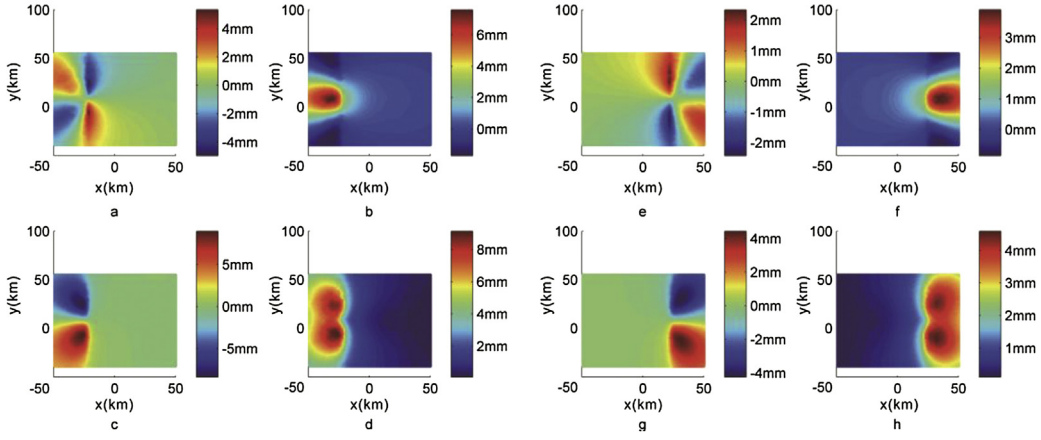

Fig. 1 – Results of subtraction.

Table 2 – Parameter values.

Group	Case	Dip angle (°)	ρ (kg/m^3)	$\mu(10^{10}$ Nm$^{-2})$		λ (10^{10} Nm^{-2})
				Hanging wall	Footwall	
1st	Case 1	60	2600.0	3.00	2.75	4.00
	Case 2	60	2600.0	2.75	2.75	4.00
	Case 3	60	2600.0	3.00	3.00	4.00
2nd	Case 1	60	2600.0	3.25	2.75	4.00
	Case 2	60	2600.0	2.75	2.75	4.00
	Case 3	60	2600.0	3.25	3.25	4.00
3rd	Case 1	60	2600.0	3.50	2.75	4.00
	Case 2	60	2600.0	2.75	2.75	4.00
	Case 3	60	2600.0	3.50	3.50	4.00
4th	Case 1	60	2600.0	3.75	2.75	4.00
	Case 2	60	2600.0	2.75	2.75	4.00
	Case 3	60	2600.0	3.75	3.75	4.00
5th	Case 1	60	2600.0	4.00	2.75	4.00
	Case 2	60	2600.0	2.75	2.75	4.00
	Case 3	60	2600.0	4.00	4.00	4.00
6th	Case 1	60	2600.0	4.25	2.75	4.00
	Case 2	60	2600.0	2.75	2.75	4.00
	Case 3	60	2600.0	4.25	4.25	4.00
7th	Case 1	60	2600.0	4.50	2.75	4.00
	Case 2	60	2600.0	2.75	2.75	4.00
	Case 3	60	2600.0	4.50	4.50	4.00
8th	Case 1	60	2600.0	4.75	2.75	4.00
	Case 2	60	2600.0	2.75	2.75	4.00
	Case 3	60	2600.0	4.75	4.75	4.00
9th	Case 1	60	2600.0	5.00	2.75	4.00
	Case 2	60	2600.0	2.75	2.75	4.00
	Case 3	60	2600.0	5.00	5.00	4.00
10th	Case 1	60	2600.0	5.25	2.75	4.00
	Case 2	60	2600.0	2.75	2.75	4.00
	Case 3	60	2600.0	5.25	5.25	4.00

X-axis and Y-axis represent the area of the area of the earthquake.

In the numerical simulation results, the impact of the medium's lateral heterogeneity caused by μ on the co-seismic deformation differ in the three directions of the surface coordinate system. In the experimental results of the 10th group, the biggest change in the X-axis, Y-axis, and Z-axis directions was 51.5 mm, 27.3 mm, and 12.2 mm, respectively. Moreover, the rate of the biggest change in the X-axis direction was more than 20%.

As shown in Table 2, the parameter of μ in the hanging wall varied from 3.0 × 10^{10} Nm^{-2} to 5.25 × 10^{10} Nm^{-2} in steps of 2.5 × 10^{9} Nm^{-2}. The co-seismic displacements were observed to increase with an increase in the μ. In addition, the increments of co-seismic displacements were not linear; they also diminished.

3.3. *Influence of fault dip angle on the impact of the medium's lateral heterogeneity*

In the neighborhood of a fault, the dip angle of the fault dominates the co-seismic displacements. For a reverse fault earthquake with high dip (60°–90°), the opposite direction

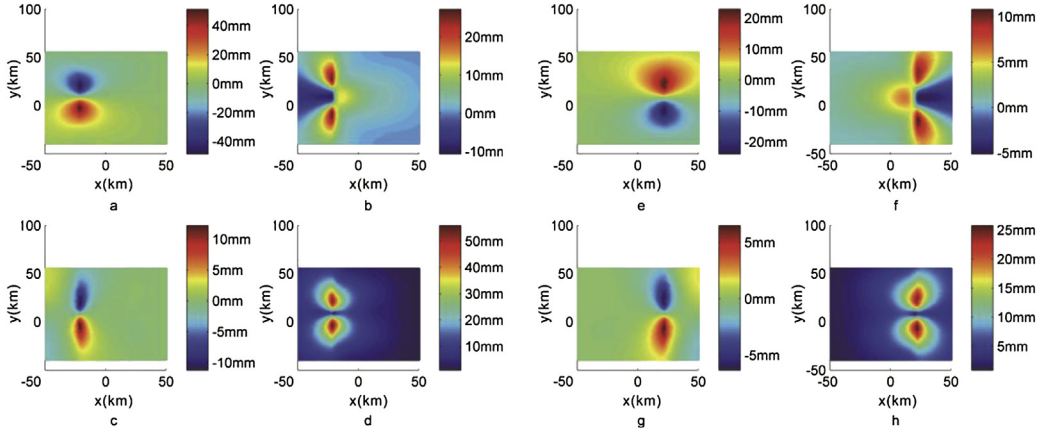

Fig. 2 – Results of subtraction.

region appears in the horizontal displacements on the hanging wall; the area of the opposite direction region increases with the dip-angle and the increase in the extent of the co-seismic displacements on the footwall is obvious [15]. The conclusions above from previous studies are useful, but the studies did not consider lateral heterogeneity. Therefore, we designed six groups of experiments to determine the influence of fault dip angle on the impact of the medium's lateral heterogeneity; these six groups are listed in Table 3.

We obtained the influence of the fault's dip angle on the impact of medium's lateral heterogeneity by subtracting as described previously, and these results are shown in Fig. 3. In the figure, the area where the X-axis is negative represents the hanging wall, and the area where the X-axis is positive represents the footwall. The Y-axis represents the impact of lateral heterogeneity on the co-seismic deformation.

As shown in Fig. 3, when the fault's dip angle is 15°, the impact of the medium's lateral heterogeneity on the hanging wall is obviously greater than the impact on the footwall. The biggest change on the hanging wall is 24.86 mm, while it is 4.42 mm for the footwall; the biggest change on the hanging wall is almost six times as big as that on the footwall. When the fault's dip angle varies from 15° to 60°, the impacts on the hanging wall and footwall both increase; the biggest change on the hanging wall is 43.47 mm, while it is 22.77 mm for the footwall; the biggest change on the hanging wall is almost twice as big as that on the footwall. When the fault's dip angle varies from 60° to 90°, the impact on the footwall increases, but diminishes on the hanging wall; the biggest changes on the hanging wall and footwall are both 35.57 mm.

3.4. *Impact of lateral heterogeneity on co-seismic deformation in the near-field and far-field*

According to Zhang [17], the constraints of the near-field area responding to Mw6.0, Mw6.5, Mw7.0, and Mw7.5 earthquakes are 25, 35, 40, 45 km, respectively. Therefore, the results obtained in this study are all in the near-field. To determine whether lateral heterogeneity has an impact on co-seismic deformation in the far-field, the following experiments designed (Table 4).

Again, the impact of the medium's lateral heterogeneity on the co-seismic deformation was determined through subtraction, and these results are shown in Fig. 4.

Fig. 4(a) Impact of lateral heterogeneity of the hanging wall on the co-seismic deformation in the X-axis direction; 4(b) Impact of the hanging wall in the Y-axis direction; 4(c) Impact of the hanging wall in the Z-axis direction; 4(d) The square root of the impact of the hanging wall in all directions; 4(e) Impact of lateral heterogeneity of the footwall on co-seismic deformation in the X-axis direction; 4(f) Impact of the footwall in the Y-axis direction; 4(g) Impact of the footwall in the Z-axis direction; 4(h) The square root of the impact of the footwall in all directions. In the figure, the units of the X- and Y-axes are in km, they

Table 3 – Parameter values.

Group	Case	Dip angle (°)	ρ (Kg/m^3)	λ (10^{10} Nm^{-2})		μ(10^{10} Nm^{-2})	
				Hanging wall	Footwall	Hanging wall	Footwall
1st	Case 1	15	2600	4.50	3.50	4.25	2.70
	Case 2	15	2600	4.50	4.50	4.25	4.25
	Case 3	15	2600	3.50	3.50	2.70	2.70
2nd	Case 1	30	2600	4.50	3.50	4.25	2.70
	Case 2	30	2600	4.50	4.50	4.25	4.25
	Case 3	30	2600	3.50	3.50	2.70	2.70
3rd	Case 1	45	2600	4.50	3.50	4.25	2.70
	Case 2	45	2600	4.50	4.50	4.25	4.25
	Case 3	45	2600	3.50	3.50	2.70	2.70
4th	Case 1	60	2600	4.50	3.50	4.25	2.70
	Case 2	60	2600	4.50	4.50	4.25	4.25
	Case 3	60	2600	3.50	3.50	2.70	2.70
5th	Case 1	75	2600	4.50	3.50	4.25	2.70
	Case 2	75	2600	4.50	4.50	4.25	4.25
	Case 3	75	2600	3.50	3.50	2.70	2.70
6th	Case 1	90	2600	4.50	3.50	4.25	2.70
	Case 2	90	2600	4.50	4.50	4.25	4.25
	Case 3	90	2600	3.50	3.50	2.70	2.70

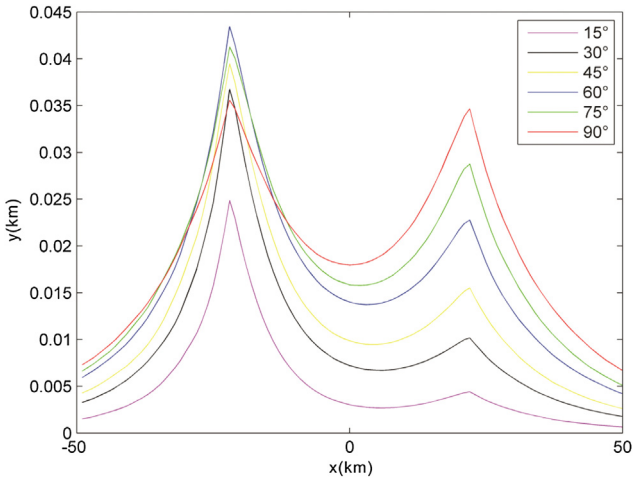

Fig. 3 – The influence of fault dip angle on the impact of lateral heterogeneity.

Table 4 – Parametervalues.

Case	Dip angle (°)	ρ (kg/m^3)	λ (10^{10} Nm^{-2})		μ (10^{10} Nm^{-2})	
			Hanging wall	Footwall	Hanging wall	Footwall
Case 1	60	2600	4.50	3.50	4.25	2.70
Case 2	60	2600	4.50	4.50	4.25	4.25
Case 3	60	2600	3.50	3.50	2.70	2.70

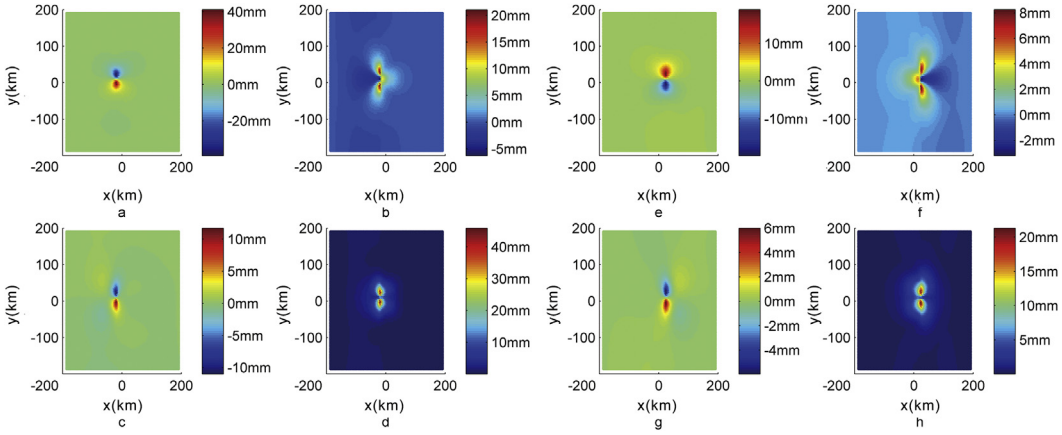

Fig. 4 – Impact of lateral heterogeneity in the near- and far-field.

represent the area of the earthquake. As shown in Fig. 4, lateral heterogeneity has a great impact on co-seismic displacements in the near-field, but little impact in the far-field.

3.5. *Impact of the medium's lateral heterogeneity on post-seismic viscoelastic deformation*

For geological evolution analysis, the viscoelastic effect plays an important role in post-seismic effect analysis and tectonic evolution simulation. The lateral heterogeneity caused by the viscosity coefficient also has an impact on the post-seismic viscoelastic deformation. To determine how lateral heterogeneity affects post-seismic viscoelastic deformation, the following experiments were designed (Table 5).

To observe the changes in the post-seismic viscoelastic relaxation effect through time, two points on the fault plane symmetry were chosen, a surface point on the left side of the fault plane and another surface point on the right side of the

Table 5 – Parameter values.

Group	Case	Crustal layering	ρ (kg/m^3)	λ (10^{10} Nm^{-2})	μ (10^{10} Nm^{-2})	Viscosity coefficient (Pas)	
						Left	Right
1st	Case 1	Upper crust	2600	3.40	3.20	–	–
		Lower crust	2800	4.00	3.80	10^{18}	10^{21}
	Case 2	Upper crust	2600	3.40	3.20	–	–
		Lower crust	2800	4.00	3.80	10^{18}	10^{18}
	Case 3	Upper crust	2600	3.40	3.20	–	–
		Lower crust	2800	4.00	3.80	10^{21}	10^{21}
2nd	Case 1	Upper crust	2600	3.40	3.20	–	–
		Lower crust	2800	4.00	3.80	10^{19}	10^{21}
	Case 2	Upper crust	2600	3.40	3.20	–	–
		Lower crust	2800	4.00	3.80	10^{19}	10^{19}
	Case 3	Upper crust	2600	3.40	3.20	–	–
		Lower crust	2800	4.00	3.80	10^{21}	10^{21}
3rd	Case 1	Upper crust	2600	3.40	3.20	–	–
		Lower crust	2800	4.00	3.80	10^{20}	10^{21}
	Case 2	Upper crust	2600	3.40	3.20	–	–
		Lower crust	2800	4.00	3.80	10^{20}	10^{20}
	Case 3	Upper crust	2600	3.40	3.20	–	–
		Lower crust	2800	4.00	3.80	10^{21}	10^{21}

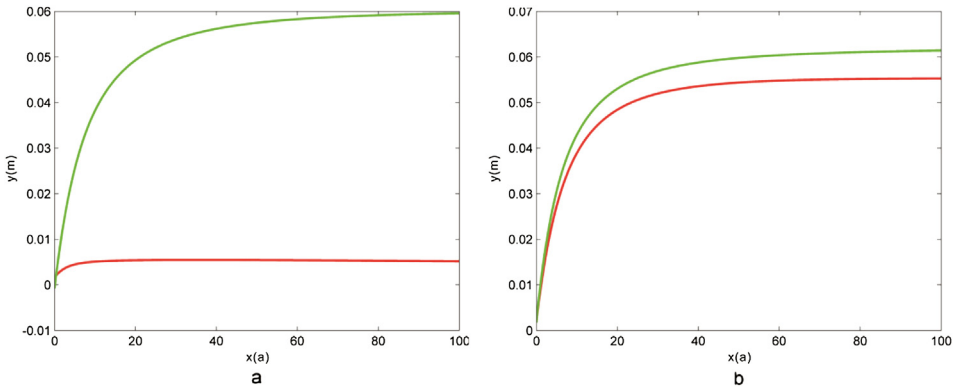

Fig. 5 – Effect of lateral heterogeneity on post-seismic viscoelastic deformation through time.

fault plane. The results are shown in Fig. 5. In Fig. 5(a), the red curve describes the post-seismic viscoelastic relaxation effect of the surface point on the right side of the fault plane in case 1 for a period of 100 years. The green curve describes the same point in case 2. In Fig. 5(b), the red curve describes the post-seismic viscoelastic relaxation effect of the surface point on the left side of the fault plane in case 1 for a period of 100 years. The green curve describes the same point in case 2. In the figure, they represent changes in the post-seismic viscoelastic relaxation effect through time.

As seen in Fig. 5, the post-seismic viscoelastic relaxation effect is mainly affected by the viscosity coefficient. In the short period after an earthquake, the post-seismic viscoelastic relaxation effect is obvious, but the effect diminishes after several years. The impact of lateral heterogeneity caused by the viscosity coefficient on post-seismic deformation is large.

To determine the impact of lateral heterogeneity caused by the viscosity coefficient, we again performed subtraction, as done previously (Figs. 6 and 7). In these figures, the X- and Y-axes represent the area of the earthquake.

As seen in Fig. 6, in the first group, the impact of lateral heterogeneity caused by the viscosity coefficient on post-seismic displacements differs in the three directions of the surface coordinate system. The biggest change in the X-axis, Y-axis, and Z-axis directions is more than 18 mm, 46 mm, and 60 mm, respectively. Moreover, the rate of the biggest change in the Z-axis direction is 56%.

As shown in Fig. 7, in the third group, the impact of lateral heterogeneity caused by the viscosity coefficient on post-seismic displacements differs in the three directions of the surface coordinate system. The biggest change in the X-axis, Y-axis, and Z-axis directions is more than 5.2 mm, 10.9 mm, and 11.5 mm, respectively. Moreover, the rate of the biggest change in the Z-axis direction is 19%.

Detailed analyses of the experimental data showed that the impact of lateral heterogeneity caused by the viscosity coefficient on post-seismic deformation increased with in the

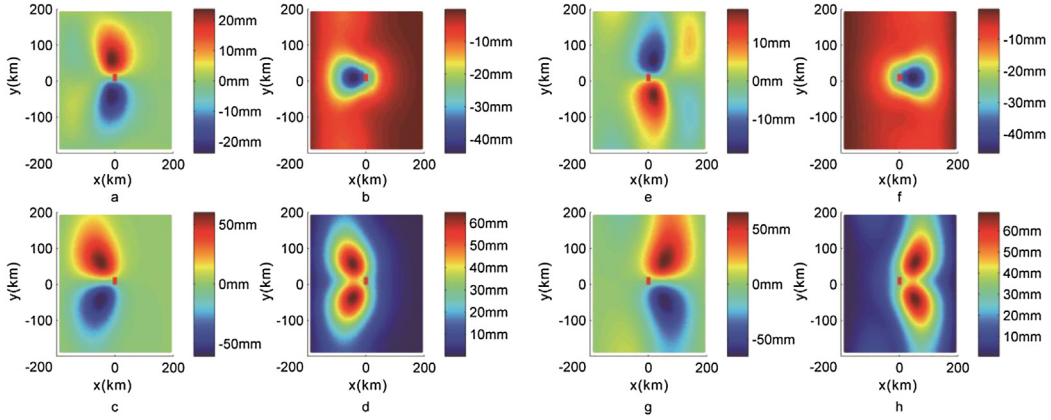

Fig. 6 – Results of subtraction. Notes: Fig. 6(a) Impact of lateral heterogeneity of the hanging wall caused by the viscosity coefficient on post-seismic deformation in the X-axis direction in the first group; 6(b) Impact of the hanging wall in the Y-axis direction; 6(c) Impact of the hanging wall in the Z-axis direction; 6(d) The square root of the impact of the hanging wall in the X- and Y-axes directions; 6(e) Impact of lateral heterogeneity of the footwall caused by the viscosity coefficient on post-seismic deformation in the X-axis direction in the first group; 6(f) Impact of the footwall in the Y-axis direction; 6(g) Impact of the footwall in the Z-axis direction; 6(g) The square root of the impact on the footwall in the X- and Y-axes directions.

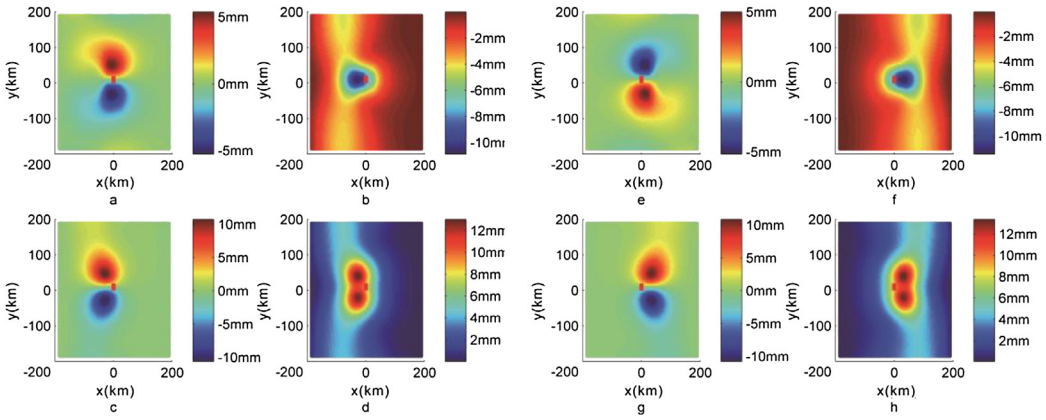

Fig. 7 – Results of subtraction. Notes: Fig. 7(a) Impact of lateral heterogeneity of the hanging wall caused by the viscosity coefficient on post-seismic deformation in the X-axis direction in the third group; 7(b) Impact of the hanging wall in the Y-axis direction; 7(c) Impact of the hanging wall in the Z-axis direction; 7(d) The square root of the impact of the hanging wall in the X- and Y-axes directions; 7(e) Impact of lateral heterogeneity of the footwall caused by the viscosity coefficient on post-seismic deformation in the X-axis direction in the third group; 7(f) Impact of the footwall in the Y-axis direction; 7(g) Impact of the footwall in the Z-axis direction; 7(h) The square root of the impact of the footwall in the X- and Y-axes directions.

lateral heterogeneity caused by the viscosity coefficient. In addition, the increments of post-seismic displacements were not linear; they were also diminishing. Moreover, the impact of lateral heterogeneity caused by the viscosity coefficient on post-seismic deformation can affect a large area, including the near- and far-field.

4. Conclusions

1) The lateral heterogeneity can affect the co-seismic displacement, and the effects increase with increase in the lateral heterogeneity caused by material parameters.
2) The Lame parameters play a more dominant role than density in the effects caused by the medium's lateral heterogeneity. μ has a greater impact on the medium's lateral heterogeneity than λ. In addition, the medium's lateral heterogeneity has a large impact on the co-seismic deformation in the near-field, but it has almost no impact on the co-seismic deformation in the far-field.
3) Fault dip angle has an effect on the medium's lateral heterogeneity; when it is smaller than 90°, the impact of the medium's lateral heterogeneity on the hanging wall is greater than on the footwall. When the fault dip angle varies from 15° to 60°, the impacts on the hanging wall and footwall both increase. When the fault dip angle varies from 60° to 90°, the impact on the footwall increases, while it diminishes on the hanging wall.
4) The post-seismic viscoelastic relaxation effect is mainly affected by the viscosity coefficient, changing according to changes in the viscosity coefficient. For a short period after an earthquake, the post-seismic viscoelastic relaxation effect is obvious, but the effect diminishes after several years. The impact of lateral heterogeneity caused by the viscosity coefficient on post-seismic deformation can affect a large area, including the near- and far-field.

Acknowledgement

This work is co-supported by the National Natural Science Foundation of China (41431069), the State Key Development Program for Basic Research of China (2013CB733304, 2013CB733303), the Doctoral Fund of Ministry of Education of China (20110141130010) and China Postdoctoral Science Foundation funded project (2013M542062).

REFERENCES

[1] Steketee JA. On Volterra's dislocations in a semi-infinite elastic medium. Can J Phys 1958;36:192–205.
[2] Chinnery MA. The deformation of ground around surface faults. Bull Seism Soc Am 1961;51:355–72.
[3] Chinnery MA. The stress changes that accompany strike-slip faulting. Bull Seism Soc Am 1963;53:921–32.
[4] Maruyama T. Static elastic dislocations in an infinite and semi-infinite medium. Bull Earthq Res Inst Univ Tokyo 1964;42:289–368.
[5] Chen Yuntai, Lin Banghui, Lin Zhongyang, Li Zhiyong. The focal mechanism of the 1966 Hsingtai earthquake as inferred from the ground deformation observation. Chin J Geophys 1975;18(3):164–82 [in Chinese].
[6] Chen Yuntai, Lin Banghui, Wang Xinhua, Huang Liren, Liu Miaolong. A dislocation model of the Tangshan earthquake of 1976 from the inversion of geodetic data. Chin J Geophys 1979;22(3):201–16 [in Chinese].

[7] Okada Y. Surface deformation due to shear and tensile faults in a half-space. Bull Seismol Soc Am 1985;75(4):1135–54.
[8] Wang R, Lorenzo-Martín F, Roth F. PSGRN/PSCMP—a new code for calculating co-and post-seismic deformation, geoid and gravity changes based on the viscoelastic-gravitational dislocation theory. Comput Geosci 2006;32(4):527–41 [in Chinese].
[9] Lou Hai. Deep tectonic setting of the 2008 Wenchuan Ms8.0 earthquake in southwest China—Joint analysis of teleseismic P-wave receiver functions and Bouguer gravity anomalies. Sci China (Series D) 2009;38(10):1207–20.
[10] Xu Caijun, Wang Hao, Jiang Guoyan. Study on crustal deformation of Wenchuan Ms8.0 earthquake using wide swath ScanSAR and MODIS. Geodesy Geodyn 2011;2(2):1–6.
[11] Wu Jianchao, Yu Song, Cai Yongjian, Lei Dongning, Li Heng. Stress triggering of the Lushan M7.0 earthquake by the Wenchuan Ms8.0 earthquake. Geod Geodyn 2013;4(3):35–9.
[12] Rybicki K. The elastic residual field of a very long strike slip fault in the presence of a discontinuity. Bull Seism Soc Am 1971;61:79–92.
[13] Rybicki K. Static deformation of a laterally inhomogeneous half-space by a two-dimensional strike-slip fault. J Phys Earth 1978;26:351–66.
[14] Rybicki K, Kasahara K. A strike-slip fault in a laterally inhomogeneous medium. Tectonophysics 1977;42:127–38.
[15] Li Feng, Huang Jinshui. Numerical simulation of influences of medium heterogeneity and dip of fault on coseismic displacement. J Geod Geodyn 2011;31(5):52–60 [in Chinese].
[16] Dziewonski AM, Anderson DL. Preliminary reference earth model. Phys Earth Planet Interiors 1981;25(4):297–356.
[17] Zhang Lei, Shi Xiaoling. Analysis of near field seism. West China Explor Eng 2005;17(1):193–4 [in Chinese].

Xu Bei (1988—), male, Master of Engineering, majors in geodetic inversion and geodetic data processing.

Xu Caijun (1964—), male, the Yangtze River scholar distinguished professor, majors in space geodesy and geophysical geodesy.